A&A 446, 301–306 (2006)
DOI: 10.1051/0004-6361:20053445


Astronomy & Astrophysics

# A periodic arcade model for extended EUV filaments

U. Anzer[1] and P. Heinzel[2,1]

[1] Max-Planck-Institut für Astrophysik, Karl-Schwarzschild-Str. 1, 85740 Garching, Germany
e-mail: ula@mpa-garching.mpg.de
[2] Astronomical Institute, Academy of Sciences of the Czech Republic, 25165 Ondřejov, Czech Republic

Received 17 May 2005 / Accepted 14 September 2005

**ABSTRACT**

The extensions of H$\alpha$ filaments that are observed in EUV spectral lines require the presence of cool material in a large volume surrounding these filaments. This material can only be supported by magnetic fields with dips. Such dips can be generated by a sufficiently strong twisting of magnetic flux tubes. In the present paper we have extended earlier work to more realistic magnetic field configurations that are periodic in the $x$-direction. We derived approximate equilibria for twisted slender flux tubes and determined the region that contains dips. In addition we investigated the effects on our models of the mass loading due to a heavy prominence. Finally we compared our theoretical models with the EUV – observations. We conclude that these types of models are capable of explaining the basic features of the observations.

**Key words.** Sun: filaments – Sun: magnetic fields – Sun: UV radiation

## 1. Introduction

The EUV extensions of solar H$\alpha$ filaments that were studied by Heinzel et al. (2001) and Schmieder et al. (2003) represent a big challenge for our theoretical understanding of these types of structures. The detailed analysis of the observations obtained by SOHO (SOlar and Heliospheric Observatory) in different EUV lines (i.e. coronal and transition-region lines) suggests that the darkening is due to a combination of absorption and blocking of these lines. In particular, the absorption mechanism requires a sufficiently high column density of neutral hydrogen and also of neutral and singly ionised helium (for details see Anzer & Heinzel 2005). Therefore cool material must exist in a region that is horizontally very extended. Then the basic problem is how any cool material can be supported in a stable way in large areas surrounding the central narrow H$\alpha$ filament. Two different ideas of how this could happen have been presented so far: the parasitic polarity model of Aulanier & Schmieder (2002) and the twisted flux tube model of Anzer & Heinzel (2003). The latter is based on the possibility that the extended EUV structures could be explained by an ensemble of sufficiently twisted flux tubes within a bipolar magnetic arcade. In that paper Anzer & Heinzel only demonstrated how the mechanism can work in theory, but they did not try to reproduce the observed structure in detail.

In our new investigation, we wanted to use more realisic arcades. In the previous study, we took an arcade where all field lines are parts of a set of concentric circles whose origine lies below the solar surface. This made the analysis particularly simple because each flux tube had a constant cross section. In addition the azimuthal field of the twisted tube, $B_\phi$, was constant along each tube. In this case, a simple criterion for kink instability could be applied. But such a configuration has some severe shortcomings: the arcade is not confined and it extends horizontally to infinity. And at large heights, the field becomes extremely flat since there the radius of curvature goes to infinity. Therefore we searched for some more realistic types of global field configurations, which will be presented in this paper.

The width of the region with magnetic dips depends strongly on the amount of twist that is present in each flux tube, therefore it is very important to estimate the maximum amount of twist allowed for such configurations. Recently two papers have appeared that deal with this problem: Török & Kliem (2003) and Gerard et al. (2004). Both numerically treat the development of a selected flux tube embedded in a bipolar magnetic region. The foot points of the flux tubes are subjected to a rotational twisting motion, and the subsequent evolution of the tubes is then followed. The results of the two investigations are somewhat different. Török & Kliem find that, during an extended period of twisting, the apex of the loop moves slowly upward to heights 2–3 times the original starting value, whereas the general shape of the loop remains unchanged. After that time, a sudden onset of a dynamical, unstable development occurs. The maximum twist reached in the stable phase amounts to $\approx$1.3. The calculation by Gerard et al. was run up to a time when the twist had a value of 1.7, after which the calculation was stopped because of accumulating large numerical errors. But at this time the limit of stability was not yet reached. Therefore in this case, the maximum allowed

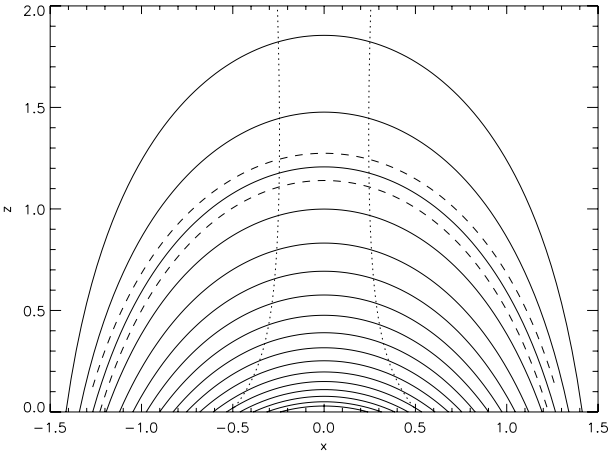


**Fig. 1.** Arcade of a potential magnetic field. The two dashed lines show the cross section of one selected flux tube. The dotted lines indicate the boundaries of the region with dips.

twist will be larger than 1.7, and there is no sign of any upward motion of the loop as a whole. The reason for this slight difference of the two sets of models could be the following: *i*) a different distribution of the local twist, or *ii*) the difference in the global bipolar field. In our present study, we took the most favourable case with a twist resulting in $n_{\max} \approx 2$ and assumed that the loops are stationary. But one has to be aware of the possibility that both these assumptions may not be entirely correct. Ignoring these uncertainties, we performed local investigations of approximate tube equilibria for tubes that are embedded in a magnetic arcade. Such approximate equilibria can be calculated analytically, as we shall demonstrate in this paper. In Sect. 2 we describe a model for extended EUV filaments based upon periodic magnetic arcades; in Sect. 3 we present our results; Sect. 4 deals with the question how the weight of the filament will modify this simple model and in Sect. 5 we offer some discussion.

## 2. Periodic arcade model

As a starting point, we take a potential field that is periodic in $x$, with a half–period $\pi$ (in dimensionless units). This field can be written as

$$B_x = B\ \cos(x)\,\mathrm{e}^{-z} \tag{1}$$

$$B_z = -B\ \sin(x)\,\mathrm{e}^{-z}, \tag{2}$$

where $B$ is the constant field strength at the solar surface, which we normalise in the following by setting $B = 1$, and the surface is placed at $z = 0$. Then the field lines can be calculated by using the flux function $F$ with

$$F = \cos(x)\,\mathrm{e}^{-z}, \tag{3}$$

which leads to

$$\cos(x)\,\mathrm{e}^{-z} = \cos(x_0), \tag{4}$$

where each field line starts at the foot point defined by $x = x_0$ and $z = 0$. Such a field is shown in Fig. 1.

One also obtains

$$B(x, z) = \mathrm{e}^{-z} \tag{5}$$

and $\alpha = x$, where $\alpha$ is the angle between the field line direction and the horizontal plane.

A new feature of this configuration is that the field strength decreases exponentially with height. Therefore all flux tubes will spread out in the $x$–$z$ plane with increasing height, but the width in $y$-direction remains constant. This means that a flux tube that has a circular cross section with radius $a_0$ at the solar surface becomes very elliptical at the top. But this happens only if the flux tube is not twisted. As soon as a certain amount of twist is present, the magnetic tension forces will lead to a cross section that is approximately circular at all heights.

This circularisation of the flux tube cross section is very efficient for flux tubes with an amount of twist that is large enough. But as we discuss in the following paragraphs, the azimuthal field $B_\phi$ is limited by the requirement that the flux tubes have to be stable against kink modes. Therefore, for all slender flux tubes, the value of $B_\phi$ has to be small. For this reason we now investigate the situation in more detail. We estimate the tension force due to the presence of $B_\phi$ and compare it to the restoring force of the potential field arcade. We denote the radii of curvature in the initially elliptical flux tube by $r_1$ for the top and bottom and by $r_2$ for the sides. Then the circularisation force will be given by

$$\delta f = \frac{B_\phi^2}{4\pi}\left(\frac{1}{r_1} - \frac{1}{r_2}\right). \tag{6}$$

For the shape of the elliptical tube, we take $r_1 = 1/2\ a$ and $r_2 = 2\ a$ at the loop apex. This then leads to the approximate relation

$$\delta f \approx \frac{B_\phi^2}{2\pi}\frac{1}{a}. \tag{7}$$

The potential field that describes the magnetic arcade is in magnetic equilibrium. Therefore the tension force has to balance the pressure gradient and both of these quantities are given by $f' = 1/4\pi\ \mathrm{e}^{-z}$. Any distortion that results from the presence of a twisted flux tube will destroy this balance. The two forces are now no longer equal, as a small difference will arise leading to a restoring force, $\delta f'$. This force is characterised by the difference between tension and pressure gradient. Therefore it will be a small fraction of $f'$. We take as an order of magnitude estimate

$$\delta f' \approx 0.3\frac{1}{4\pi}\mathrm{e}^{-z}. \tag{8}$$

Now considering the appex of a flux tube with $z_{\mathrm{top}} = 1$, we find

$$\delta f' \approx \frac{0.1}{4\pi}. \tag{9}$$

The condition for the circularisation, $\delta f > \delta f'$, gives the minimum value of $B_\phi$ needed:

$$B_\phi^2 > 0.05a. \tag{10}$$

As is shown towards the end of this section, the maximum twist that is allowed for a stable flux tube leads to the estimates given

by the Eqs. (26), (31), and (33). Taking $a = a_0$ and $l = 3$, we can then estimate the maximum azimuthal field as

$$B_\phi \approx 0.16. \tag{11}$$

The critical value for $B_\phi$ resulting from Eq. (10) is

$$B_{\phi\,\mathrm{cr}} = \sqrt{0.002} \approx 0.04. \tag{12}$$

These estimates show that all flux tubes that are twisted to their stability limit experience a strong circularisation effect. Therefore from now on we use only flux tubes with circular cross sections, which simplifies the analysis considerably.

To describe the physical conditions in the flux tube, we now introduce a local cylinrical coordinate system denoted by $(r, \phi, s)$, where $s$ measures the distance along the tube, and the tube radius is given by $r_0 = a(s)$. For the thin flux tubes considered in this investigation, we assume that the field inside the tube can be approximated locally by a straight cylinder. The field in this cylinder has to be force free. As a particularly simple force-free configuration, we take here the field first considered by Gold & Hoyle (1960), which we adopt to our special situation and write it in the following way:

$$B_s(s, r) = B_1(s)\left(1 + \left(\frac{B_{\phi 0}(s)}{B_1(s)}\frac{r}{a(s)}\right)^2\right)^{-1} \tag{13}$$

and

$$B_\phi = B_{\phi 0}\frac{r}{a(s)}\left(1 + \left(\frac{B_{\phi 0}(s)}{B_1(s)}\frac{r}{a(s)}\right)^2\right)^{-1}. \tag{14}$$

This field has the following properties: $B_s(s, 0) = B_1(s)$, $B_\phi(s, 0) = 0$, $B_s(s, a(s)) = B_1(s)(1 + B_{\phi 0}(s)/B_1(s))^2 \equiv B_2(s)$, and $B_\phi(s, a(s)) \approx B_{\phi 0}(s)$.

The flux tube has to be embedded into the magnetic arcade. At the boundary between the tube and the arcade the field has a discontinuity, which gives rise to a current sheet. This current represents the return current of the twisted flux tube. In principle, one could imagine that the current sheet is smeared out, but for convenience we only consider this simplified configuration. The only condition that we impose is that, at the boundary between the flux tube and the surrounding arcade field, the magnetic pressure has to be continuous. This leads to the relation

$$B_{\phi 0}^2(s) + B_2^2(s) = B^2 \tag{15}$$

where $B$ is the field strength of the arcade at the position $s$ of the flux tube.

An additional condition is the requirement that the azimuthal force in the flux tube vanishes, which is equivalent to the vanishing of the magnetic torque. This condition can be written in the form

$$\frac{1}{4\pi r}\left(B_r\frac{\partial}{\partial r}(rB_\phi) + B_s\frac{\partial}{\partial s}(rB_\phi)\right) = 0. \tag{16}$$

Here we make use of the cylindrical symmetry of the flux tube with $\partial/\partial\phi = 0$. This last equation requires that the quantity $rB_\phi$ remains constant along each field line. This then gives rise to the relation

$$B_{\phi 0}(s) = B_0\frac{a_0}{a(s)}. \tag{17}$$

In order to indicate that, for the slender flux tubes considered in this investigation, the azimuthal component of the field will be rather small, we now set

$$B_0 = \epsilon \tag{18}$$

with $\epsilon \ll 1$. An additional constraint is the conservation of the magnetic flux inside the tube, where this flux is given by the relation

$$\Phi = 2\pi\int_0^{a(s)} B_s(r, s) r\mathrm{d}r. \tag{19}$$

Using Eq. (13), we get

$$\Phi \approx 2\pi B_1(s)\int_0^{a(s)}\left(1 - \left(\frac{B_{\phi 0}(s)}{B_1(s)}\right)^2\frac{r^2}{a^2(s)}\right) r\mathrm{d}r \tag{20}$$

which then leads to

$$\Phi \approx \pi B_1(s) a^2(s)\left(1 - \frac{1}{2}\left(\frac{B_{\phi 0}(s)}{B_1(s)}\right)^2\right). \tag{21}$$

To the lowest order in $B_{\phi 0}/B$, we have the approximate relations

$$B_2(s) \approx B\left(1 - \frac{1}{2}\left(\frac{B_{\phi 0}(s)}{B}\right)^2\right) \tag{22}$$

and

$$1 + \frac{1}{2}\left(\frac{B_{\phi 0}(s)}{B_1(s)}\right)^2 \approx 1 + \frac{1}{2}\left(\frac{B_{\phi 0}(s)}{B}\right)^2. \tag{23}$$

This gives us

$$\Phi \approx \pi a^2(s) B \tag{24}$$

which is accurate up to the order of $\epsilon^2$. Applying this condition to the lower boundary where $a(0) = a_0$ and $B = 1$, we then get from flux conservation the equation

$$\frac{a(s)}{a_0} \approx \frac{1}{\sqrt{B}}. \tag{25}$$

As a next step we calculate the total twist at the surface of the flux tube. For that we use the relation

$$n = 2\int_0^{s_0}\frac{B_{\phi 0}(s)}{2\pi a(s) B_2(s)}\mathrm{d}s \tag{26}$$

where $s_0$ denotes the position of the top of the tube and the total length will be 2 $s_0$. The quantity $n$ gives the number of turns along the entire flux tube. Taking Eqs. (17) and (22), one obtains

$$n \approx 2\epsilon B\int_0^{s_0}\frac{a_0}{2\pi a^2(s) B\left(1 - \left(B_{\phi 0}(s)/B\right)^2/2\right)}\mathrm{d}s. \tag{27}$$

For the arcade field along the flux tube as given by Eq. (4) we have

$$B = \frac{\cos(x_0)}{\cos(x)}. \tag{28}$$

Together with the equation for d$s$

$$\mathrm{d}s = \frac{\mathrm{d}x}{\cos(x)} \tag{29}$$

we obtain the relation

$$n \approx \frac{\epsilon}{\pi a_0} \int_0^{x_0} \left( \frac{1}{\cos(x)} + \frac{1}{2}\epsilon^2 \frac{1}{\cos(x_0)} \right) \mathrm{d}x. \tag{30}$$

The integration then gives

$$n \approx \frac{\epsilon}{\pi a_0} \left( \frac{l}{2} + \frac{1}{2}\epsilon^2 \frac{x_0}{\cos(x_0)} \right) \tag{31}$$

where the quantity $l$ represents the length of the flux tube with

$$l = 2 \ln \left[ \tan\left( \frac{x_0}{2} + \frac{\pi}{4} \right) \right]. \tag{32}$$

If we now take for $n$ the value of 2, which is the limit for stability, then to lowest order in $\epsilon$ one has the estimate

$$\epsilon \approx \frac{2\pi a_0}{\ln\left[ \tan\left( \frac{x_0}{2} + \frac{\pi}{4} \right) \right]}. \tag{33}$$

As a next step, we calculate the extension of the region in which the twisting of the flux tube produces dips of the field lines. The condition for this is that the vertical component of the azimuthal field produced by the twist is larger than the vertical component of the original longidudinal field. For simplicity, we again only consider the field at the outer boundary of the flux tube. Then the boundary of the dip region is obtained by setting the two field components equal to each other, which gives

$$B_{\phi 0} \cos(x_1) \approx B_2 \sin(x_1), \tag{34}$$

where $x_1$ now denotes the position of this boundary. We also have used the relation $\alpha = x_1$. Making use of Eqs. (17), (22), and (25), we then obtain in lowest order in $\epsilon$

$$\epsilon \sqrt{\frac{\cos(x_0)}{\cos(x_1)}} \cos(x_1) \approx \frac{\cos(x_0)}{\cos(x_1)} \sin(x_1). \tag{35}$$

This leads to the relation

$$\epsilon^2 (\cos(x_1))^3 \approx \cos(x_0) - \cos(x_0)\,(\cos(x_1))^2. \tag{36}$$

Taking again only the lowest order terms in $\epsilon$, we finally arrive at the relation that defines $x_1$

$$\cos(x_1) \approx 1 - \frac{1}{2}\frac{\epsilon^2}{\cos(x_0)} \tag{37}$$

and, from the equation that defines the field lines, we get the height, $z_1$, of the boundary as

$$z_1 = \ln\left[ \frac{\cos(x_1)}{\cos(x_0)} \right]. \tag{38}$$

These equations then allow us to determine the region in the arcade that has dips and that therefore can be directly related to the EUV-extensions.

**Table 1.** Geometry of the dip region.

| $x_0$/km | $\epsilon$ | $x_1$/km | $z_1$/km |
|---|---|---|---|
| 25 000 | 0.47 | 24 000 | 1000 |
| 35 000 | 0.32 | 18 000 | 11 000 |
| 50 000 | 0.20 | 14 000 | 32 000 |
| 70 000 | 0.09 | 13 000 | 110 000 |

## 3. Size of EUV-extensions

To obtain the true dimesions of these regions, we first have to specify a geometrical length scale. For this we assume that the full width of the arcade amounts to 150 000 km, therefore each polarity region is 75 000 km wide. This then implies that the non-dimensional value of 1 corresponds approximately to 50 000 km. As in the paper by Anzer & Heinzel (2003), we take $a_0 = 2000$ km for the radius of the flux tube at the solar surface, or $a_0 = 0.04$ in non-dimensional units. With these values, we calculate the extension of the dip region. The results are shown in Table 1 and in Fig. 1.

Taking a flux tube radius $a_o = 2000$ km leads, together with a typical flux tube length $L = 150\,000$ km, to an aspect ratio $L/a_0$ of 75. This value is much larger than those considered in the numerical calculations of Török & Kliem (2003) and of Gerard et al. (2004), which range between 5 and 15. This means that the flux tubes considered by these authors are much fatter than those entering into our modelling. This will also imply that resolving our flux tubes numerically would require a grid that is 10 times finer than presently used, and this would present a tremendous numerical task. Therefore, at the moment, the stability estimates for our models can only proceed by extrapolations from results obtained for thicker flux tubes.

From the table we see that $x_1$ ranges from 24 000 km at the bottom to 13 000 km at very large heights. Therefore the full width ranges between 26 000 km and 48 000 km. These widths have to be compared with the ones of the EUV-extensions as measured by Schmieder et al. (2003), who quote maximum values around 70 000 km. A comparison with our theoretical values indicates that the model can at least give the right size in the order of magnitude, although the width is systematically somewhat too small.

There are several mechanisms that could produce a wider dip area: (*i*) the magnetic arcade itself could be wider, (*ii*) the flux tube has a larger radius, or (*iii*) the weight of the prominence can shift the peaks of the field lines to the sides. The last mechanism is the most interesting, and we shall discuss it in detail in the next section.

## 4. Effects resulting from the weight of the prominence

If the prominence is sufficiently heavy, then the central parts of the magnetic arcade will be pulled down, and a new configuration results with two peaks and one central dip. Under these circumstances the dips produced by the flux tube twisting will be centred around the two peaks on the sides of the prominence. If we make the simplifying assumption that the

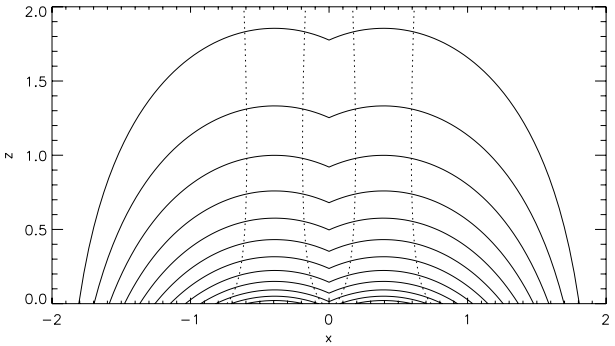


**Fig. 2.** Double-peaked magnetic arcade. The current sheet at $x = 0$ represents the massive prominence. The dotted lines give the boundaries of the two regions with dips.

prominence itself is modelled by a current sheet, then we can construct a simple analytical model based on the periodic field configuration discussed in the previous sections.

Such a configuration can be obtained in the following way: for $x > 0$ the arcade described above is shifted to the right by an amount of $\Delta x$, and for $x < 0$ it is shifted to the left by the same amount. Then the new arcade extends from $-(\pi/2 + \Delta x)$ to $(\pi/2 + \Delta x)$. The configuration resulting from this procedure is shown in Fig. 2. For our particular field, the inclination of the field lines at the prominence, $\alpha_\mathrm{p}$, is given by the relation

$$\alpha_\mathrm{p} = \pm\Delta x. \tag{39}$$

For $0 \le x \le \pi/2 + \Delta x$, the new field is given by

$$B_x = \cos(x - \Delta x)\,\mathrm{e}^{-z} \tag{40}$$

$$B_z = -\sin(x - \Delta x)\,\mathrm{e}^{-z}, \tag{41}$$

with the flux function $F$ as

$$F = \cos(x - \Delta x)\,\mathrm{e}^{-z}, \tag{42}$$

which results in the equation for the field lines

$$\cos(x - \Delta x)\,\mathrm{e}^{-z} = \cos(x_0 - \Delta x). \tag{43}$$

Since the field has to be symmetric with respect to the $z$-axis, the field line equation for the entire region is given by

$$\cos(|x| - \Delta x)\,\mathrm{e}^{-z} = \cos(x_0 - \Delta x), \tag{44}$$

where $x_0$ and $\Delta x$ are positive quantities.

As before, the number of turns of the twisted flux tubes can be obtained from Eqs. (26) to (32).

For the total number of turns along a flux tube that passes through the prominence, one finds

$$n \approx \frac{\epsilon}{\pi a_0}\int_0^{x_0}\left(\frac{1}{\cos(x - \Delta x)} + \frac{1}{2}\epsilon^2\frac{1}{\cos(x_0 - \Delta x)}\right)\mathrm{d}x, \tag{45}$$

which gives

$$n \approx \frac{\epsilon}{\pi a_0}\left(\frac{l}{2} + \frac{1}{2}\epsilon^2\frac{x_0}{\cos(x_0 - \Delta x)}\right), \tag{46}$$

where the full length of the flux tube is now given by

$$l = 2\left\{\ln\left[\tan\left(\frac{x_0 - \Delta x}{2} + \frac{\pi}{4}\right)\right] + \ln\left[\tan\left(\frac{\Delta x}{2} + \frac{\pi}{4}\right)\right]\right\}. \tag{47}$$

Assuming again $n = 2$ and considering only the lowest order in $\epsilon$, we arrive at the relation

$$\epsilon \approx \frac{2\pi a_0}{\ln\left[\tan\left(\frac{x_0 - \Delta x}{2} + \frac{\pi}{4}\right)\right] + \ln\left[\tan\left(\frac{\Delta x}{2} + \frac{\pi}{4}\right)\right]}. \tag{48}$$

The approximate position of the boundary of the dip region, $x_1$, is now obtained by the relation

$$\cos(x_1 - \Delta x) \approx 1 - \frac{1}{2}\frac{\epsilon^2}{\cos(x_0 - \Delta x)}. \tag{49}$$

If we want to determine the boundary in physical units, we have to perform the correct scaling. In this new case, the arcade extends from $x = -(\pi/2 + \Delta x)$ to $x = \pi/2 + \Delta x$. Therefore the full width of the arcade is $\pi + 2\Delta x$. For the inclination of the prominence field, we take a value of 22.5 deg, or $\pi/8$. Then the dimensionless length of $5\pi/4$ will correspond to 150 000 km, which we take for the arcade dimension as before. With these values and using Eqs. (34) to (38), we finally arrive at a maximum extension of the dip region of 32 000 km, or a total width of 64 000 km. This is almost the same as the values quoted by Schmieder et al. (2003).

In this calculation, we have assumed that the stabilising of the flux tubes is only due to the freezing-in at the photosphere. But the massive prominence itself could also have some stabilising influence. If the prominence is at rest, then the length determining the kink stability will be reduced by a factor 1/2, and $\epsilon$ can therefore be twice as large. This additional effect will widen the dip region even more.

So far we have only considered the 2 extreme cases: (*i*) the prominence mass loading is negligible, and (*ii*) there is a heavy loading.

But the situation will be more complex in reality, because of the prominence fine stucture. Heinzel & Anzer (2001) have modelled this behaviour by assuming a series of vertical threads. In this case there will be a superposition of loaded and unloaded flux tubes, and the overall configuration can be described best by a mixture of flux tubes, which were presented in this and the previous sections. The result will be that the dip region can be very extended.

## 5. Discussion

We have constructed magnetic field models that can explain some of the basic aspects of EUV-filament extensions. Our analytical model is based upon an ensemble of very slender flux tubes embedded into a potential field arcade. This configuration is only approximately in magnetic equilibrium. Some exact equilibrium configurations of this type were calculated numerically by Török & Kliem (2003) and by Gerard et al. (2004). But in their models, the flux tubes were about a factor 10 wider than those taken for our configurations. These tubes are therefore too wide for our purposes. A further shortcoming of these numerical approaches is that they give the solution only for one single case. Therefore one cannot derive the overall shape of the dip region in this way. We found that our models are capable of producing the right horizontal extensions of the regions with dips, and they also give acceptable heights for the structures.

Therefore we consider this approach as very promising. There are, however, still some open questions about this modelling.

We took a particularly simple geometry of the underlying prominence field, and used a potential field arcade without any shear. This is an oversimplification, since prominences generally show a strongly sheared magnetic field. Shearing will stretch the flux tubes and thus make them longer. Therefore the allowed values for $B_\phi$ will be smaller, which leads to a reduction of the width of the dip region. We shall postpone the investigation of such configurations to a future paper. Another problem is that our models have normal polarity, whereas the majority of the quiescent prominences have inverse polarity. But at present, it is not yet clear what an appropriate model for *I*-polarity prominences would be. So far models based upon giant flux ropes, quadrupolar configurations, or fields that have very extreme values for the magnetic shear all have been suggested in the literature. Because of this uncertainty, and also the complexity of all such models, we cannot say anything about the extensions of *I*-polarity prominences at present.

The other open question concerns the mass loading of the individual magnetic dips. The presence of dips is a neccessary condition for the EUV-extensions, but we cannot predict how much cool mass will typically be present in each dip. We can, however, give some statistical estimates. We assume that a certain fraction, $f$, of the EUV-extension region is filled with cool gas. We further suggest that the cool structures extend over approximately one pressure scale-height and that at the boundary to the corona (along each flux tube), the gas pressure is equal to the coronal value. If we take $T = 10^6$ K and $n_\mathrm{e} = n_\mathrm{p} = 10^8$ cm$^{-3}$ for the corona and assume for the cool structures $T = 10^4$ K and an ionisation degree of 1/2, then pressure equilibrium gives a neutral hydrogen density of $0.7 \times 10^{10}$ cm$^{-3}$. The mean value over one pressure scale height will amount to $10^{10}$ cm$^{-3}$. From the investigations of Schwartz et al. (2004), one finds an optical thickness at 912 Å that is larger than 1 (a representative value would be 5) and a vertical extension around 25 000 km. This optical thickness will require a column density of neutral hydrogen around $8 \times 10^{17}$ cm$^{-2}$. This column density can be produced by an ensemble of cool stuctures that fill a certain fraction $f$ of the total volume of the EUV extension. By taking for the vertical extension 25 000 km we can then determine the filling factor $f$. With the numbers given above, we get $f = 0.03$, or 3% of the extended EUV region volume. If the filling is similar in all three spatial dimensions, we find for the one – dimensional filling a value of around 0.3. This seems quite a reasonable result. On this basis, we conclude that such multiple dip configurations are capable of reproducing the observations.

The model developed in the last section is only partially applicable. It assumes that the heavy prominence extends to infinite heights, but in reality prominences will typically reach heights of several tens of thousands of km. Therefore above such heights, the double-peak structure of the field should disappear. A more realistic model therefore should go smoothly from the double-peak structures at the bottom to one with a single peak at large heights. But configurations of this type cannot be treated in a simple, analytical way. Therefore on the basis of our previous modelling we propose that the lower parts should be described by Eqs. (43) and (49), whereas the upper parts should be given by Eqs. (37) and (38), with some appropriate transition between the two regimes. Such a combined model will have rather promising aspects. It can produce a total width of around 60 000 km at the bottom and results in widths of less than 10 000 km above 60 000 km. These properties are in good agreement with the results obtained by Schwartz et al. (2004).

*Acknowledgements.* The authors thank the referee for the very helpful criticism that lead to this new, improved version of the paper. SOHO is a space mission of international cooperation between ESA and NASA. This work was partially supported by the ESA-PECS project No. 98030.

## References

Anzer, U., & Heinzel, P. 2003, A&A, 404, 1139
Anzer, U., & Heinzel, P. 2005, ApJ, 622, 714
Aulanier, G., & Schmieder, B. 2002, A&A, 386, 1106
Gerard, C. L., Hood, A. W., & Brown, D. S. 2004, Sol. Phys., 222, 79
Gold, T., & Hoyle, F. 1960, MNRAS, 120, 89
Heinzel, P., & Anzer, U. 2001, A&A, 375, 1082
Heinzel, P., Schmieder, B., & Tziotziou, K. 2001, ApJ, 561, L223
Schmieder, B., Tziotziou, K., & Heinzel, P. 2003, A&A, 401, 361
Schwartz, P., Heinzel, P., Anzer, U., & Schmieder, B. 2004, A&A, 421, 323
Török, T., & Kliem, B. 2003, A&A, 406, 1043